Optical absorption in ultrathin silicon oxide films near the SiO_2/Si interface

Naozumi Terada, Takashi Haga, Noriyuki Miyata,* and Kazunori Moriki
Department of Electrical and Electronic Engineering, Musashi Institute of Technology, Setagaya-ku, Tokyo 158, Japan

Masami Fujisawa
Institute for Solid State Physics, The University of Tokyo, 3-2-1 Midori-cho, Tanashi 188, Japan

Mizuho Morita and Tadahiro Ohmi
Department of Electronics, Tohoku University, Sendai 980, Japan

Takeo Hattori
Department of Electrical and Electronic Engineering, Musashi Institute of Technology, Setagaya-ku, Tokyo 158, Japan
(Received 25 February 1992)

The optical absorption in ultrathin silicon oxide films was studied by measuring their reflectance spectra in the vacuum ultraviolet. By applying a modified Kramers-Kronig analysis, with multiple reflections at the boundaries of the film taken into account, depth profiling was performed of the optical absorption in the oxide films near the SiO_2/Si interface below the fundamental absorption edge of fused quartz. The structural imperfections contributing to this optical absorption were found to arise partly from Si-Si bonds localized within a distance of 1.4 nm from the interface in the oxide films.

I. INTRODUCTION

According to studies on the transmittance spectra of nearly 50-nm-thick silicon thermal oxide films,[1,2] the absorption coefficients in the vacuum ultraviolet were found to coincide with those calculated from the optical constants of fused quartz. However, the optical absorption in SiO_2/Si interfacial transition region cannot be determined from these studies alone. The reason is that the interfacial transition region was removed along with the silicon substrate by the chemical etching at the time that the substrate was selectively etched off in order to obtain a silicon oxide film supported by a silicon substrate at the periphery of the silicon oxide film for a transmittance measurement. Therefore nondestructive measurements, such as a reflectance measurement, are necessary for detection of optical absorption in the interfacial transition region. Philipp and Taft[3] pointed out that silicon oxide films having thicknesses of less than 3 nm formed on a silicon substrate exhibit large changes in the reflectance with thickness change in the photon-energy range 8.5–12 eV. In particular, they showed that the existence of ultrathin thermal oxide films has an appreciable effect on the reflectance in the vacuum ultraviolet. Furthermore, they found that the reflectance spectrum of a 2.6-nm-thick native oxide film formed on a silicon substrate was different from that of a thermal oxide film formed on a silicon substrate with the same thickness in the photon-energy range 8.5–12 eV. In particular, they found that the reflectance was affected strongly by the deviation in composition of the native oxide film from that of the thermal oxide film.

However, the dependence of the optical properties on the oxide film thickness cannot be determined from the reflectance spectrum alone because the reflectance of ultrathin silicon oxide films is affected strongly by the thickness change.[3] Thus, the modified Kramers-Kronig relation derived by Lupashiko, Miloslavskii, and Shklyarevskii,[4] which takes into account the effect of multiple reflections at the boundaries of the film, was used to analyze the reflectance spectra in order to determine the optical constants of the silicon oxide films.[5–7] For this analysis, it is necessary to determine the complex frequency at which the complex reflectance becomes zero. Because the complex reflectance cannot be determined from the measurement, the complex frequency was determined for a silicon oxide film with thickness t as follows:[5–7] The complex frequency is determined for a quartz film with thickness t. Then the complex frequency is adjusted near this complex frequency so that the measured spectrum satisfies the modified Kramers-Kronig relation. Based on preliminary studies[5–7] on the reflectance of ultrathin thermal oxide films, optical absorption due to Si-Si bonds in the oxide film near the interface has been found.

Near the SiO_2/Si interface, both compositional and structural transition regions exist. By using surface-sensitive techniques, such as photoelectron spectroscopy, the thickness of a compositional transition layer[8] was found to be in the range 0.3–0.6 nm, while that of a structural transition layer[9] was found to be in the range 3–7 nm. In the compositional transition region, suboxides were detected.[8]

It is the purpose of the present paper to clarify the chemical structures of compositional and structural transition layers from the analysis of the reflectance spectrum. First, the method used to determine the optical-absorption coefficients of thermal-oxide film from the

 ©1992 The American Physical Society

reflectance spectrum is described in detail. Second, the measurements on the change in reflectance caused by the change in thickness are described. These measurements are analyzed to determine the change in optical properties as a function of depth. It is shown that a decrease in thickness results in an increase in the absorption coefficients below the fundamental absorption edge of fused quartz. The origin of this optical absorption near the interface is shown to arise from suboxides existing in the oxide film near the interface.

II. EXPERIMENTAL DETAILS

After removing nearly 200-nm-thick oxide films by advanced buffered hydrogen fluoride (HF 3.7 wt. %, NH_4F 20 wt. %), which were formed on 3-Ωcm *p*-type (100)-oriented CZ silicon wafers in dry oxygen at 1000 °C, successively thinner oxides were grown in dry oxygen at 800 °C by an ultraclean oxidation method.[10] Reflectance measurements were performed on as-grown oxide films with thicknesses of 1.9, 4.5, 7.1, 9.1, and 12.3 nm and on oxide films with thicknesses of 1.4, 2.7, and 3.5 nm obtained from the chemical etching of 4.5-nm-thick thermal-oxide films. The chemical etching was performed using dilute HF ([HF]:[CH_3OH]:[H_2O]=1:18:1) with ultrasonic vibration of the solution. Transmittance measurement was performed on a 50.5-nm-thick thermal-oxide film. This oxide film was prepared by removing silicon substrate in two steps. In the first step, the substrate was etched by anisotropic etching[11,12] until the thickness of the substrate reached 1 μm. In the second step, the silicon substrate was etched off by XF_2.[13] The thickness of silicon oxide films, except for 50.5-nm-thick silicon oxide film, were determined from the ratio of (N_O/N_S).[14] Here, N_O and N_S are the Si 2*p* spectral intensities for silicon in silicon dioxide and for silicon in the silicon substrate, respectively. Surface Science Instruments SSX-100 furnished with monochromatized Al $K\alpha$ radiation was used to measure highly resolved Si 2*p* photoelectron spectra. The values of electron escape depths in a silicon substrate and in silicon thermal oxide are 2.7 and 3.4 nm, respectively. These electron escape depths were determined from the oxide film thickness dependence of (N_O/N_S). The thickness of the thermal-oxide film used for transmittance measurement was deduced from the analysis of the transmittance spectrum.

The measurement of reflectance was carried out at Beam Line 1 of the 0.38 GeV SOR ring of the Institute for Solid State Physics by using a 1-m Seya-Namioka-type monochromator in the photon energy range 5–23 eV. The monochromatic light, which was incident on the silicon oxide film with an incident angle of 10°, was polarized in the plane of incidence. Since the reflectance is weakly affected by the optical constants of silicon oxide film in the photon-energy range 5.1–5.4 eV, the absolute values of reflectance could be determined and the refractive index of thermally grown silicon oxide films found to be equal to that of fused quartz[15] in this photon-energy range. This was confirmed by the fact that the absolute value of reflectivity shown in Fig. 1, which was measured by using a Shimadzu MPC-300 in the photon-energy

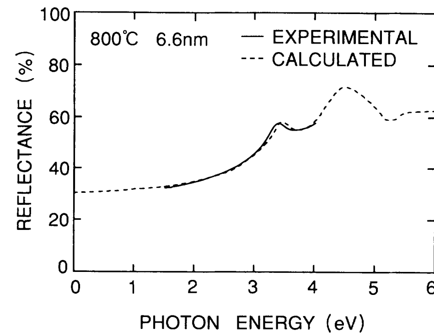

FIG. 1. Solid line shows the absolute value of reflectivity measured for 6.6-nm-thick thermal-oxide film formed in dry oxygen at 800 °C. The dashed line shows the reflectivity of fused quartz (Ref. 15).

range 1.5–4 eV, almost coincides with that calculated from optical constants of fused-quartz[15] and single-crystal silicon.[16]

III. ANALYSIS OF THE REFLECTANCE SPECTRUM

In order to determine the optical constants of silicon oxide film grown thermally on single-crystal silicon from the reflectance spectrum alone, it is necessary to determine the phase change on reflection from the Kramers-Kronig analysis of reflectance in the photon-energy range zero to infinity. Then, after describing the method of extrapolation of reflectivity beyond the photon-energy range studied, a modified Kramers-Kronig analysis that takes into account multiple reflections at the boundaries of the film is described.

As shown in Fig. 2, the sample studied is assumed to consist of a silicon thermal oxide film with a complex index of refraction N_1 and thickness t and a silicon substrate with a complex index of refraction N_2. Then, reflection coefficient r_{012} at normal incidence is given by

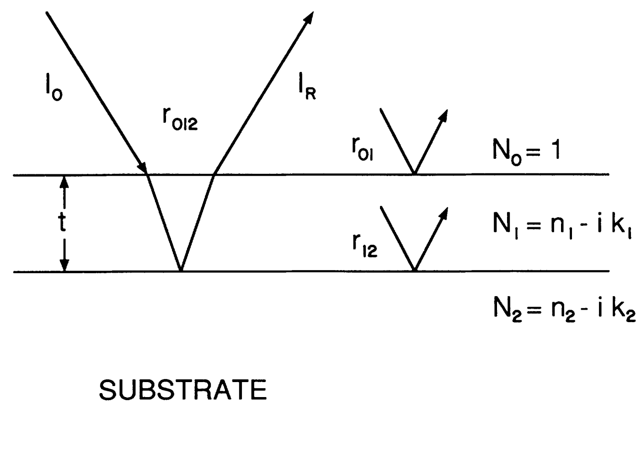

FIG. 2. Schematic diagram of the oxidized silicon surface idealized as a single layer of material with thickness t.

the following equation:

$$r_{01}=\frac{N_0-N_1}{N_0+N_1}\ ,$$

$$r_{12}=\frac{N_1-N_2}{N_1+N_2}\ ,$$

$$r_{012}=\frac{r_{01}+r_{12}\exp(-2i\delta_1)}{1+r_{01}r_{12}\exp(-2i\delta_1)}=R^{1/2}\exp(i\phi)\ .$$

Here, λ is the wavelength of incident light and $\delta_1=(2\pi/\lambda)N_1 t$. Therefore, in order to determine the complex index of refraction of silicon oxide film, the phase change on reflection ϕ is necessary in addition to reflectivity R.

A. Extrapolation of the reflectance spectrum

The reflectance spectrum beyond the photon-energy range studied was determined as follows. The reflectance spectrum in the photon-energy range 0–5.1 eV is calculated by using optical constants of fused-quartz[15] and single-crystal silicon.[16] The connection of this reflectance spectrum to measured reflectance spectra is already described in the preceding section. Furthermore, the reflectance spectrum in the photon energy larger than 23 eV is calculated by assuming that real and imaginary parts of the complex dielectric constant of single-crystal silicon and silicon thermal oxide can be approximated by the following equations:[17]

$$\epsilon_1=n^2-k^2=\epsilon_\infty-\frac{\omega_p^2\tau^2}{\omega^2\tau^2+1}$$

and

$$\epsilon_2=2nk=\frac{\omega_p^2\tau}{\omega(\omega^2\tau^2+1)}\ .$$

Here, n and k are respectively, the real and imaginary parts of the complex index of refraction. ω and ω_p are the angular frequency and angular plasma frequency, respectively. τ is a momentum relaxation time constant. In the case of single-crystal silicon, the values of ω_p and τ are determined such that optical constants determined from these equations coincide with those of single-crystal silicon in the photon-energy range 23–23.5 eV. In the case of oxide film grown thermally on single-crystal silicon, the values of ω_p and τ are determined such that the reflectance calculated using these expressions coincides with the measured spectrum in the photon-energy range 22–23 eV. The values of $\hbar\omega_p$ and τ used for the description of optical constants of single-crystal silicon are 16.5 eV and 1.02×10^{-15} s, respectively. On the other hand, the values of $\hbar\omega_p$ and τ used for the description of optical constants of oxide film grown thermally on single-crystal silicon depends weakly on the oxide film thickness such that the value of $\hbar\omega_p$ is in the range 26.2–27.9 eV and the value of τ is in the range 6.54×10^{-15}–8.57×10^{-14} s. The existence of a plasma resonance in the oxide film is plausible because bulk- and surface-loss functions of slightly oxidized silicon surfaces are quite similar to those of single-crystal silicon.[18]

B. Phase change on reflection

According to Lupashiko, Miloslavskii and Shklyarevskii,[4] the phase change on reflection at normal incidence can be given by the following modified Kramers-Kronig relation, which includes the effect of multiple reflections at the boundaries of the film:

$$\phi(\omega_i)=\left[\pi+\frac{\omega_i}{\pi}\int_0^\infty\frac{\ln[R(\omega_i)/R(\omega)]}{\omega^2-\omega_i^2}d\omega\right]-2\left\{\sum_{m=0}^{n-1}\left[\arctan\left[\frac{y_m}{x_m-\omega_i}\right]-\arctan\left[\frac{y_m}{x_m+\omega_i}\right]\right]\right\}$$
$$\equiv\phi_1(R)+\phi_2(x_m,y_m)\ .$$

Here, $R(\omega)$ is the reflectivity at frequency ω and $\phi(\omega_i)$ is the phase change on reflection at frequency ω_i. The complex reflectivity is defined such that the real frequency ω in the real reflectivity is replaced by a complex frequency, $\hat{\omega}$. x_m and y_m are the real and imaginary parts of $\hat{\omega}_m$, at which complex reflectivity becomes zero; in other words, $\ln[R(\omega_i)/R(\hat{\omega}_m)]$ becomes infinity. This $\hat{\omega}_m$ is denoted as a branch point.[4] n is the number of branch points. ϕ_2 arises from a phase change on multiple reflection at the boundaries of the silicon oxide film.

C. Determination of branch points

Because the branch points (x_m,y_m) cannot be determined from the reflectivity measured, the branch points were first determined for the fused-quartz film on single-crystal silicon. In particular, the phase change on reflection ϕ_f is determined by substituting optical constants of fused-quartz[15] and single-crystal silicon[16] in the expression of reflection coefficient r_{012}. In Fig. 3, the dependence of phase change ϕ_f on photon energy for 6.0-nm-thick fused-quartz film on single-crystal silicon is shown in addition to ϕ_1 obtained by applying a Kramers-Kronig analysis to the reflectance calculated from the op-

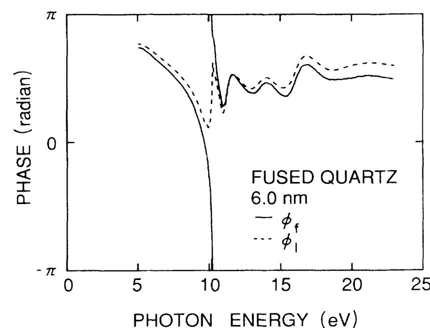

FIG. 3. Dependence of phase change on reflections ϕ_f and ϕ_1 on photon energy for 6-nm-thick fused-quartz film.

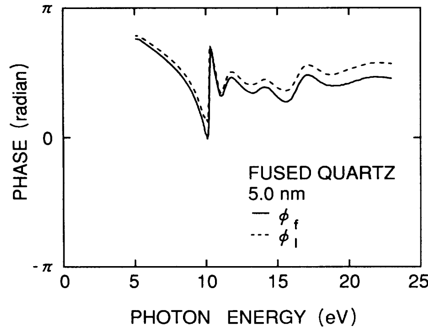

FIG. 4. Dependence of phase change on reflections ϕ_f and ϕ_1 on photon energy for 5-nm-thick fused-quartz film.

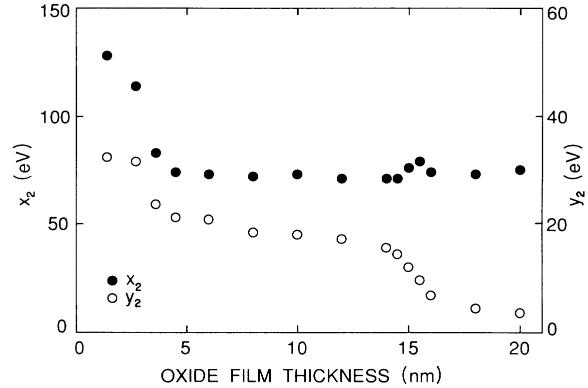

FIG. 6. Dependence of values of the second branch point on oxide film thickness.

tical constants of fused-quartz[15] and single-crystal silicon.[16] By performing the same kind of calculation of the phase change on reflection, the photon-energy dependences of ϕ_f and ϕ_1 shown in Fig. 4 are obtained for 5.0-nm-thick fused-quartz film on single-crystal silicon. Because Fig. 3 exhibits an abrupt change near the photon energy of 10 eV, the branch point must be located near 10 eV. Specifically, the branch point (x_{f1}, y_{f1}) is determined such that the photon-energy dependence of ϕ is close to that of ϕ_f. However, the photon-energy dependence of ϕ_f in Fig. 3 cannot be explained by only one branch point. Therefore, another branch point (x_{f2}, y_{f2}) is assumed at a higher photon energy. The phase change calculated by using these two branch points coincides extremely well with ϕ_f. Applying the same kinds of calculations of phase changes on reflection for fused-quartz films with various thicknesses, $n=1$ is found for fused-quartz film with a thickness ≤ 5.2 nm, while $n=2$ is found for fused-quartz film with thickness between 5.3 and 36 nm. The thickness dependence of branch points (x_{f1}, y_{f1}), (x_{f2}, y_{f2}) thus determined are shown in Figs. 5 and 6.

The phase change on reflection for an oxide film with thickness t was then calculated by substituting the reflectance spectrum of the oxide film and branch points for a fused-quartz film with thickness t into the modified Kramers-Kronig relation. The deviation of this phase change from the phase change for the fused-quartz film with thickness t was minimized in the photon-energy range 5.1–5.4 eV by changing the values of branch points near those for fused-quartz film. This procedure is equivalent to the assumption that the optical constants of oxide film are equal to those of fused-quartz film below the photon energy of 5.4 eV; in other words, optical absorption arising from structural imperfections in the oxide film is negligible below the photon energy of 5.4 eV.

From the branch points thus determined and the measured reflectance spectrum, the optical constants of thermal-oxide films were determined.

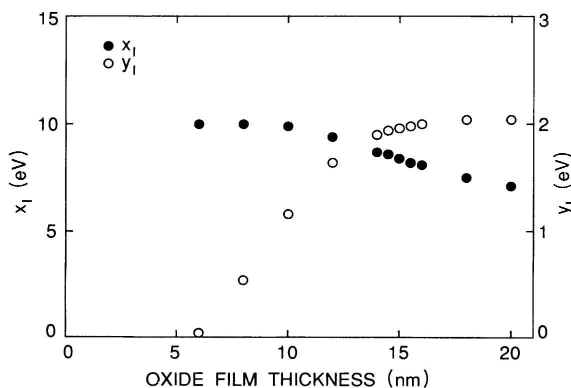

FIG. 5. Dependence of values of the first branch point on oxide film thickness.

IV. EXPERIMENTAL RESULTS AND DISCUSSION

A. Reflectance spectrum

The change in the reflectance spectrum of 4.5-nm-thick silicon oxide films with a decrease in oxide film thickness is shown in Fig. 7. The dashed lines in this figure are cal-

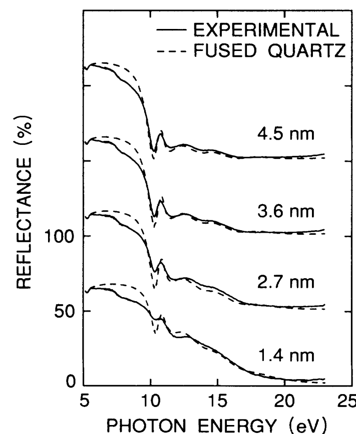

FIG. 7. Change in the reflectance spectrum with decrease in oxide film thickness. 3.6-, 2.7- and 1.4-nm-thick thermal-oxide film was obtained by chemical etching of 4.5-nm as-grown thick thermal-oxide film.

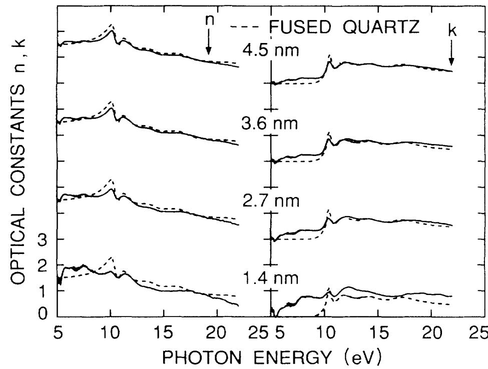

FIG. 8. Solid lines are optical constants calculated from reflectance spectra of oxide films used for Fig. 7 and dashed lines are optical constants of fused-quartz film.

culated for the reflectance of fused-quartz films whose thicknesses are equal to those of the thermal-oxide films. It can be seen from this figure that the difference in the reflectance between a thermal-oxide film and a fused-quartz film is appreciable, especially in the photon-energy range 6–9 eV.

B. Optical constants

The solid lines in Fig. 8 show the photon-energy dependence of the optical constants determined by the procedure described in the preceding section. The dashed lines in this figure indicate the optical constants of fused quartz. It can be seen from this figure that the difference in optical constants between a thermal-oxide film and a fused-quartz film increases with decreasing thickness, especially in the photon-energy range 6–9 eV.

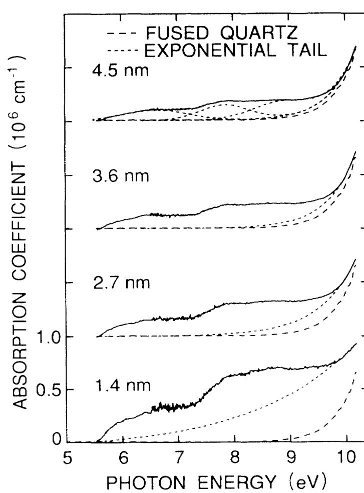

FIG. 9. Solid lines show the changes in the absorption spectra, which are calculated from optical constants of thermal-oxide film shown in Fig. 8, with decrease in oxide film thickness. Dashed lines show the absorption spectrum of fused quartz. Dotted lines show the exponential absorption tail. Deconvoluted spectra are shown for 4.5-nm oxide film.

C. Absorption coefficients

The solid lines in Fig. 9 show the photon-energy dependence of the optical-absorption coefficients calculated from the optical constants of silicon oxide films shown in Fig. 8. The dashed lines in this figure show the optical-absorption coefficient of fused quartz. In order to show the change in absorption coefficients as a function of depth, the difference in absorption coefficients $\Delta\alpha$ between two oxide film thickness are calculated using the relation $\Delta\alpha=(\alpha_2 t_2-\alpha_1 t_1)/(t_2-t_1)$ and are shown in Fig. 10, that is, the difference in the absorption coefficient for 4.5- and 3.6-nm-thick thermal oxide, that for 3.6- and 2.7-nm-thick thermal oxide, and that for 2.7- and 1.4-nm-thick thermal oxide. Here, α_2 and α_1 are the absorption coefficient of oxide film with thickness t_2 and t_1, respectively. It can be seen from this figure that the structural imperfections in the oxide film contributing to optical absorption all exist within a distance of 1.4 nm from the interface.

Because the optical-absorption tail of fused quartz can be approximated by an exponential function, the so-called Urbach tail, the optical-absorption tails of the oxide films in Fig. 9 were approximated by the exponential function. The subraction of such optical-absorption tails from the optical absorptions in Fig. 9, followed by a deconvolution, results in three absorption bands with Gaussian line shapes located at 6.5, 7.8, and 8.8 eV. An example of such deconvolution is shown in Fig. 9 for a 4.5-nm-thick oxide film. Therefore, the deviation of the optical-absorption tail shown by dotted lines from that for fused quartz is appreciable for a 1.4-nm-thick oxide film.

Extensive studies have been previously performed on the optical absorption of bulk silica glasses below the fundamental absorption edge.[15,19–23] The existence of an optical-absorption band due to Si-Si bonds in silicon dioxide was theoretically predicted[24] and was detected in silica glass,[25] which was prepared by the chemical-vapor-deposited (CVD) soot method and subsequently dehy-

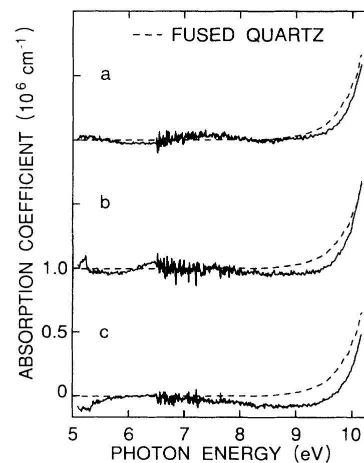

FIG. 10. Difference in absorption spectra for (a) 3.6- and 4.5-nm-thick oxide films, (b) 2.7- and 3.6-nm-thick oxide films, (c) 1.4- and 2.7-nm-thick oxide films.

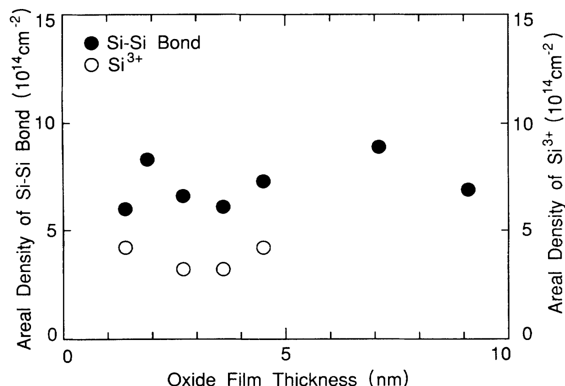

FIG. 11. Areal density of Si-Si bonds at the interface estimated from optical absorption and areal density of Si^{3+} estimated from the Si 2p photoelectron spectrum.

drated by chlorine gas treatment before sintering the CVD soot. This optical-absorption band[25] appears at 7.6 eV, which is close to the energy gap of 7.7 eV for the σ-σ^* transition of the Si-Si bond,[24] and has an optical-absorption cross section of 8×10^{-17} cm^2. Based on these studies, the absorption near 7.8 eV is ascribed to Si-Si bonds in the oxide film. The optical-absorption band at 6.5 eV was detected in the transmittance spectrum of silicon oxide,[26] which was obtained by oxidizing single-crystal silicon film on sapphire, and was considered to originate from Si-Si-Si bonds in the oxide film. It is plausible that optical-absorption band at 8.8 eV may be correlated with the Si-O-O-Si bond, whose optical absorption at 8.6 eV is theoretically predicted by O'Reilly and Robertson.[24]

The dependence of the number of Si-Si bonds on the oxide film thickness can be calculated using the relation $N=\alpha t/\sigma$ and is shown in Fig. 11. Here, N is the number density of Si-Si bonds in the oxide film, σ is the optical-absorption cross section, α is the absorption coefficient, and t is the thickness. This figure implies that Si-Si bonds with an areal density of 8×10^{14} cm^{-2} localize in the oxide film within a distance of 1.4 nm from the interface. Furthermore, the areal density of the Si-Si bonds in chemically etched films is nearly the same as that in

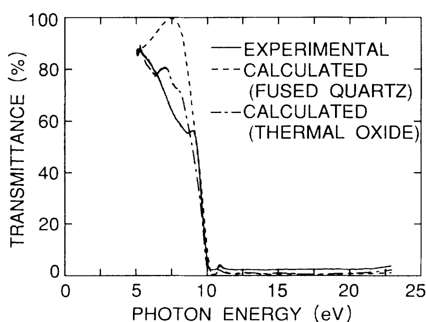

FIG. 12. Solid line and dashed line show transmittance spectra for 50.5-nm-thick thermal-oxide film and 50.5-nm-thick fused-quartz film, respectively. A dashed-dotted shows transmittance spectrum for 50.5-nm-thick thermal-oxide film calculated by using optical constants of 12.3-nm-thick thermal-oxide film.

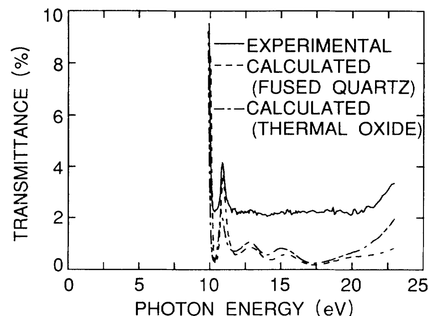

FIG. 13. Enlarged view of Fig. 12.

as-grown oxide films. Therefore, the Si-Si bonds detected are not produced by the chemical etching.

D. Transmittance spectrum

The solid line in Fig. 12 shows the transmittance spectrum for a 50.5-nm-thick thermal-oxide film, while the dashed line in this figure shows the transmittance spectrum for a 50.5-nm-thick fused-quartz film, and the dashed-dotted line in this figure shows the transmittance spectrum for a 50.5-nm-thick thermal-oxide film calculated using optical constants of a 12.3-nm-thick thermal-oxide film. Therefore, the measured transmittance spectrum observed can be roughly explained by the optical constants determined from the reflectance spectrum of the 12.3-nm-thick thermal-oxide film. Furthermore, it can be seen from Fig. 13 that strong absorption at 10.3 eV is clearly observed for silicon thermal oxide, which was observed in fused quartz[15] and was also theoretically explained.[27]

E. Si 2p photoelectron spectra

The change in the Si $2p_{3/2}$ photoelectron spectrum of a 4.5-nm-thick silicon oxide film with a decrease in the ox-

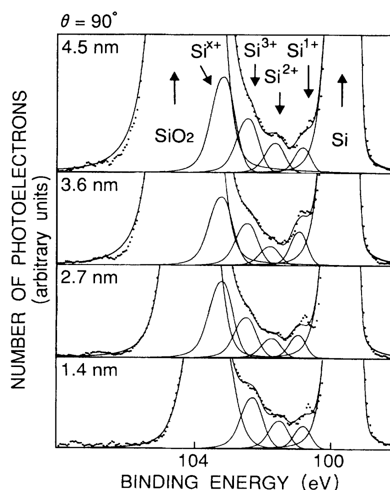

FIG. 14. Si $2p_{3/2}$ photoelectron spectra for oxide films used in Fig. 7. Deconvoluted spectra are also shown.

ide film thickness measured using ESCA-300 is shown in Fig. 14. These spectra were measured at a photoelectron takeoff angle of 90° with an acceptance angle of 3.3°. The method of removing the Si $2p_{1/2}$ spin-orbit partner from the measured spectra is almost the same as that used by Hollinger and Himpsel.[28] The deconvoluted spectra shown in this figure were obtained by assuming that the spectrum denoted by Si^{1+},Si^{2+},Si^{3+} has almost the same chemical shift and bonding configuration as that determined by Himpsel *et al.*[29] and the spectrum denoted by Si^{x+} has almost the same chemical shift and bonding configuration as that determined by Sugiyama *et al.*[30] Here, the spectral intensities for silicon in the silicon substrate are adjusted to be equal to each other. Because the Si^{3+} spectral intensity divided by the spectral intensity of silicon in the silicon substrate depends weakly on the oxide film thickness, Si^{3+} must be mostly localized near the SiO_2/Si interface.[14] Therefore, if it is assumed that Si^{3+} is localized in a silicon oxide film near the interface, the amounts of Si^{3+} determined from these deconvoluted spectra shown in Fig. 11 are obtained. The amounts of Si^{3+} determined with the same assumption for the 1.9-, 7.1-, and 9.1-nm-thick silicon oxide films are also shown in Fig. 11. Because a Si-Si bond consists of two Si^{3+}, a large difference exists between the amount of Si^{3+} estimated from optical absorption and that estimated from the Si 2p photoelectron spectrum. This difference implies the existence of unknown structural imperfections contributing to the optical absorption at 7.8 eV and is the subject of further study.

V. CONCLUSION

The reflectance spectra of silicon thermal-oxide films with thicknesses in the range 1.4–12.3 nm were measured in the photon-energy range 5–23 eV. By applying a modified Kramers-Kronig analysis to these spectra, with multiple reflections at the boundaries of the film taken into account, the change in the optical properties of thermal-oxide films as a function of depth was clarified. Namely, the thickness dependence of the optical absorption below the fundamental absorption edge of fused quartz indicates that the structural imperfections contributing to optical absorption localize in the oxide film within a distance of 1.4 nm from the interface. The optical absorption appears at 7.8 eV and is attributed to the existence of Si-Si bonds in the thermal-oxide film within a distance of 1.4 nm from the interface. The areal density of these Si-Si bonds is 8×10^{14} cm^{-2} and is larger than that estimated from the analysis of Si 2p photoelectron spectra. The optical absorption in the photon-energy range 6–9 eV was confirmed from the measurement of transmittance of a nearly 50-nm-thick thermal-oxide film.

ACKNOWLEDGMENT

One of the authors (T.H.) expresses his thanks to Dr. Masatake Katayama of SEH Isobe R&D Center for supplying silicon wafers used in the present study. A part of this work was supported by a Grant-in-Aid for Specially Promoted Research (No. 01065003) from the Ministry of Education, Science and Culture of Japan.

*Present address: Fujitsu Laboratories Ltd., Atsugi, Morinosato-Wakamiya, Atsugi, Kanagawa 243-01, Japan.

[1] R. J. Powell and M. Morad, J. Appl. Phys. **49**, 2499 (1978).
[2] Z. A. Weinberg, G. W. Rubloff, and E. Bassous, Phys. Rev. B **19**, 3107 (1979).
[3] H. R. Philipp and E. A. Taft, J. Appl. Phys. **53**, 5224 (1982).
[4] E. A. Lupashiko, V. K. Miloslavskii, and In N. Shklyarevskii, Opt. Sepctrosc. **29**, 419 (1970).
[5] N. Miyata, K. Moriki, M. Fujisawa, M. Hirayama, T. Matsukawa, and T. Hattori, Jpn. J. Appl. Phys. **28**, L2072 (1989).
[6] N. Miyata, K. Moriki, M. Fujisawa, M. Hirayama, T. Matsukawa, and T. Hattori, Solid State Electron. **33**, 327 (1990).
[7] T. Haga, N. Miyata, K. Moriki, M. Fujisawa, T. Kaneoka, M. Hirayama, T. Matsukawa, and T. Hattori, Jpn. J. Appl. Phys. **29**, L2398 (1990).
[8] *The Physics and Chemistry of SiO_2 and the $SiSiO_2$ Interface,* edited by C. R. Helms and B. E. Deal (Plenum, New York, 1988).
[9] T. Hattori, H. Yamagishi, N. Koike, K. Imai, and K. Yamabe, Appl. Surf. Sci. **41/42**, 416 (1990).
[10] M. Morita, T. Ohmi, and E. Hasegawa, Solid State Electron. **33**, 143 (1989), and references therein.
[11] R. M. Finne and D. L. Klein, J. Electrochem. Soc. **114**, 965 (1967).
[12] E. Bassous and E. F. Baran, J. Electrochem. Soc. **125**, 1321 (1978).
[13] H. F. Winters and J. W. Coburn, Appl. Phys. Lett. **34**, 70 (1979).
[14] T. Suzuki, M. Muto, M. Hara, K. Yamabe, and T. Hattori, Jpn. J. Appl. Phys. **25**, 544 (1986).
[15] H. R. Philipp, J. Phys. Chem. Solids **32**, 1935 (1971).
[16] H. R. Philipp, J. Phys. **43**, 2835 (1972).
[17] H. Ehrenreich and H. R. Philipp, Phys. Rev. **128**, 1622 (1962).
[18] H. Ibach and J. E. Rowe, Phys. Rev. B **10**, 710 (1974).
[19] E. W. J. Mitchell and E. G. S. Paige, Philos. Mag. **1**, 1085 (1956).
[20] T. W. Hickmott, J. Appl. Phys. **42**, 2543 (1971).
[21] E. Hozenkampfer, F. W. Richter, J. Stuke, and U. Voget-Grote, J. Non-Cryst. Solids **32**, 327 (1979).
[22] T. W. Hickmott, J. Appl. Phys. **45**, 1050 (1974).
[23] A. Kalnitsky, J. P. Ellul, A. R. Boothroyd, and R. S. Abbott, J. Electron. Mater. **19**, 131 (1990).
[24] E. P. O'Reilly and J. Robertson, Phys. Rev. B **27**, 3780 (1983).
[25] H. Imai, K. Arai, H. Imagawa, H. Hosono, and Y. Abe, Phys. Rev. B **38**, 12 772 (1988); H. Hosono, Y. Abe, H. Imagawa, H. Imai, and K. Arai, *ibid.* **44**, 12 043 (1991).
[26] K. Awazu, H. Kawazoe, and K. Muta, J. Appl. Phys. **70**, 69 (1991).
[27] S. T. Pantelides, in *The Physics of SiO_2 and its Interfaces,* edited by S. T. Pantelides (Pergamon, New York, 1978), p, 80.
[28] G. Hollinger and F. J. Himpsel, Appl. Phys. Lett. **44**, 93 (1984).
[29] F. J. Himpsel, F. R. McFeely, A. Taleb-Ibrahimi, and J. A. Yarmoff, Phys. Rev. B **38**, 6084 (1988).
[30] K. Sugiyama, T. Igarashi, K. Moriki, Y. Nagasawa, T. Aoyama, R. Sugino, T. Ito, and T. Hattori, Jpn. J. Appl. Phys. **29**, L2401 (1990).